COMPUTER ASSISTED PROOF OF SPURIOUS EIGENSOLUTION FOR ANNULAR AND ECCENTRIC MEMBRANES

I-Lin Chen*, Jeng-Tzong Chen**, ***, Wei-Ming Lee****, and Shang-Kai Kao**

Key words: spurious eigenvalue, degenerate kernel, doubly connected problem, null-field integral equation.

ABSTRACT

Spurious eigensolutions in the boundary integral equation (BIE) or boundary element method (BEM) for doubly-connected domain problems, the eccentric and annular membranes, are studied analytically and numerically in this paper. For the mathematical analysis, we employ the null-field integral equation, the degenerate kernels and the Fourier series to prove the existence of spurious eigensolutions in the continuous system. Examples of eccentric case, annular membrane and general shape are solved by using the null-field equation approach and BEM, respectively. Base on the numerical experiment, computer-assisted proof for the existence of spurious eigenvalues in comparison with the trivial outer boundary data is given. The spurious eigenvalue is found to be the true eigenvalue of a circular membrane with the inner radius. The SVD structure for the four influence matrices is examined. Also, the trivial outer boundary densities are found in case of spurious eigenvalues and are shown in the bar chart.

I. INTRODUCTION

Rank deficiency in BIEM or BEM appears in the spurious eigensolution for the Helmholtz problems [3, 6, 8] as well as degenerate scales in Laplace problems [5, 9]. Spurious eigensolution and fictitious frequency stem from non-uniqueness problems. They appear in different aspects in computational mechanics. First of all, hourglass modes in the finite element method (FEM) using the reduced integration occur due to rank deficiency [18]. Also, loss of divergence-free constraint for the incompressible elasticity also results in spurious modes. In the other side of numerical solution for the differential equation using the finite difference method (FDM), the spurious eigenvalue also appears due to discretization [12, 14, 21]. In the real-part BEM [4, 15] or the multiple reciprocity method (MRM) formulation [10, 11, 19, 20], spurious eigensolutions occur in solving eigenproblems. Even though the complex-valued kernel is adopted, the spurious eigensolution also occurs for the multiply-connected problem [8] as well as the appearance of fictitious frequency for the exterior acoustics [2]. In the recent work, Chen *et al.* [3, 6, 8] investigated the spurious eigenvalue for the multiply connected (annular) problems by using the degenerate kernels, the Fourier series and the null-field integral equation in a continuous system, using the degenerate kernels and circulant in a discrete system. Kuttler [16] used a conformal mapping by using the power method for lower bounds and Rayleigh-Ritz method for upper bounds for the eccentric annulus problem. In this paper, an annular region and eccentric case are considered for the eigenequation in both continuous and discrete systems. However, rigorous proof for the existence of the spurious eigensolutions for eccentric membrane was not studied before. A computer assisted proof will be done here.

In this paper, we focus on the analytical study for the existence of spurious eigenvalue for eccentric membranes in BIEM. The occurring mechanism of spurious eigenvalue is studied analytically by using the degenerate kernels and the Fourier series in the null-field integral equation and is verified numerically from the bar chart of unitary vector of SVD [7, 13]. Three treatments, the SVD updating term, the Burton & Miller method [1] and the CHIEF concept (Combined Helmholtz Interior integral Equation Formulation) [17] have been applied to filter out the spurious solution. This paper will focus on two points. One is the proof of existence for the spurious eigensolution of eccentric membranes. The other is to show the trivial outer boundary mode in the bar chart. Numerical examples by changing the eccentricity are considered to see how spurious eigenvalue change. The SVD structures for the four influence matrices in dual BEM are also examined. The results are also compared with those of BEM. Besides, a general shape problem is solved by using BEM.

Author for correspondence: Jeng-Tzong Chen (e-mail: jtchen@mail.ntou.edu.tw).
**Department of Naval Architecture, National Kaohsiung Marine University, Kaohsiung, Taiwan.*
***Department of Harbor and River Engineering, National Taiwan Ocean University, Keelung, Taiwan.*
****Department of Mechanical and Mechanical Engineering, National Taiwan Ocean University, Keelung, Taiwan.*
*****Department of Mechanical Engineering, China Institute of Technology, Taipei, Taiwan.*

II. DERIVATION OF THE OCCURRING MECHANISM OF SPURIOUS EIGENVALUES

1. Problem Statement

The governing equation of the membrane problem is the Helmholtz equation

$$(\nabla^2 + k^2)u(x) = 0, \quad x \in D^I \tag{1}$$

where ∇^2, k and D^I are the Laplacian operator, the wave number, and the domain of interest, respectively. The eccentric problem is shown in Fig. 1.

2. Dual Boundary Integral Formulation – the Conventional BEM Version

The dual boundary integral equations of the domain point are shown below:

$$2\pi u(x) = \int_B T(s,x)u(s)dB(s) - \int_B U(s,x)t(s)dB(s), \quad x \in D^I, \tag{2}$$

$$2\pi t(x) = \int_B M(s,x)u(s)dB(s) - \int_B L(s,x)t(s)dB(s), \quad x \in D^I, \tag{3}$$

where s and x are the source and field points, respectively, $t(s)$ is the directional derivative of $u(s)$ along the outer normal direction at s. The kernel function $U(s,x)$ is the fundamental solution which satisfies

$$(\nabla^2 + k^2)U(x,s) = \delta(x-s) \tag{4}$$

where $\delta(x - s)$ denotes the Dirac-delta function, $U(s,x)$, $T(s,x)$, $L(s,x)$ and $M(s,x)$ represent the four kernel functions [3, 6, 8] as

$$U(s,x) = \frac{-i\pi H_0^{(1)}(kr)}{2}, \tag{5}$$

$$T(s,x) = \frac{\partial U(s,x)}{\partial n_s} = \frac{-ik\pi H_1^{(1)}(kr)}{2}\frac{y_i n_i}{r} \tag{6}$$

$$L(s,x) = \frac{\partial U(s,x)}{\partial n_x} = \frac{ik\pi H_1^{(1)}(kr)}{2}\frac{y_i \bar{n}_i}{r} \tag{7}$$

$$M(s,x) = \frac{\partial^2 U(s,x)}{\partial n_s \partial n_x} = \frac{-ik\pi}{2}\left[-k\frac{H_2^{(1)}(kr)}{r^2}y_i y_j n_i \bar{n}_j + \frac{H_1^{(1)}(kr)}{r} n_i \bar{n}_i\right], \tag{8}$$

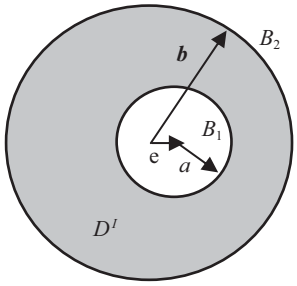

$a = 0.5\ m$
$b = 2.0\ m$
e = 0.0 ~ 1.0 m
Boundary condition:
Outer circle: $u_2 = 0$
Inner circle : $u_1 = 0$

Fig. 1. A fixed-fixed membrane with one circular hole of radius 0.5 *m*.

where $H_n^{(1)}(kr)$ is the nth order Hankel function of the first kind, $i^2 = -1$, $r = |x - s|$, $y_i = s_i - x_i$, n_i and $\bar{n}_i$ are the i^{th} components of the outer normal vectors at s and x, respectively. Equations (2) and (3) are referred to singular and hypersingular boundary integral equations (BIEs), respectively. By moving the field point x to the boundary, the dual boundary integral equations for the boundary point can be obtained as follows:

$$\pi u(x) = C.P.V.\int_B T(s,x)u(s)dB(s) - R.P.V.\int_B U(s,x)t(s)dB(s), \quad x \in B, \tag{9}$$

$$\pi t(x) = H.P.V.\int_B M(s,x)u(s)dB(s) - C.P.V.\int_B L(s,x)t(s)dB(s), \quad x \in B, \tag{10}$$

where *R.P.V.* is the Riemann principal value, *C.P.V.* is the Cauchy principal value and *H.P.V.* is the Hadamard (or call Mangler) principal value. By moving the field point to the complementary domain, the dual boundary integral equations for the boundary point can be obtained as follows:

$$0 = \int_B T(s,x)u(s)dB(s) - \int_B U(s,x)t(s)dB(s), \quad x \in D^c, \tag{11}$$

$$0 = \int_B M(s,x)u(s)dB(s) - \int_B L(s,x)t(s)dB(s), \quad x \in D^c, \tag{12}$$

where the D^c denotes the complementary domain.

3. Null-Field Integral Formulation – the Present Version

By introducing the degenerate kernels, the collocation point can be located on the real boundary without facing singularity. Therefore, the representations of integral equations including the boundary can be written as

$$2\pi u(x) = \int_B T(s,x)u(s)dB(s) - \int_B U(s,x)t(s)dB(s), \quad x \in D \cup B, \tag{13}$$

$$2\pi t(x) = \int_B M(s,x)u(s)dB(s) - \int_B L(s,x)t(s)dB(s), \quad x \in D \cup B, \tag{14}$$

and

$$0=\int_B T(s,x)u(s)dB(s)-\int_B U(s,x)t(s)dB(s),\quad x\in D^C\cup B, \tag{15}$$

$$0=\int_B M(s,x)u(s)dB(s)-\int_B L(s,x)t(s)dB(s),\quad x\in D^C\cup B, \tag{16}$$

once the kernel is expressed in terms of an appropriate degenerate form. It is found that the collocation point is categorized to the three regions, domain (Eqs. (2)-(3)), boundary (Eqs. (9)-(10)) and complementary domain (Eqs. (11)-(12)) in the conventional formulation. After using the degenerate kernel for the null-field BIEM, Eqs. (13)-(14) and (15)-(16) can contain the boundary point. The *U, T, L* and *M* kernel, can be expressed in terms of degenerate kernels as shown below [3, 6, 8]:

$$U(s,x)=\begin{cases} U^I(s,x)=\displaystyle\sum_{n=0}^{\infty}\frac{\varepsilon_n\pi}{2}\left[-iJ_n(kR)+Y_n(kR)\right]J_n(k\rho) \\ \qquad \cos(n(\theta-\phi)),\ R\ge\rho, \\ U^E(s,x)=\displaystyle\sum_{n=0}^{\infty}\frac{\varepsilon_n\pi}{2}\left[-iJ_n(k\rho)+Y_n(k\rho)\right]J_n(kR) \\ \qquad \cos(n(\theta-\phi)),\ R<\rho, \end{cases} \tag{17}$$

$$T(s,x)=\begin{cases} T^I(s,x)=\displaystyle\sum_{n=0}^{\infty}\frac{\varepsilon_n k\pi}{2}\left[-iJ_n'(kR)+Y_n'(kR)\right]J_n(k\rho) \\ \qquad \cos(n(\theta-\phi)),\ R>\rho, \\ T^E(s,x)=\displaystyle\sum_{n=0}^{\infty}\frac{\varepsilon_n k\pi}{2}\left[-iJ_n(k\rho)+Y_n(k\rho)\right]J_n'(kR) \\ \qquad \cos(n(\theta-\phi)),\ R<\rho, \end{cases} \tag{18}$$

$$L(s,x)=\begin{cases} L^I(s,x)=\displaystyle\sum_{n=0}^{\infty}\frac{\varepsilon_n k\pi}{2}\left[-iJ_n(kR)+Y_n(kR)\right]J_n'(k\rho) \\ \qquad \cos(n(\theta-\phi)),\ R>\rho, \\ L^E(s,x)=\displaystyle\sum_{n=0}^{\infty}\frac{\varepsilon_n k\pi}{2}\left[-iJ_n'(k\rho)+Y_n'(k\rho)\right]J_n(kR) \\ \qquad \cos(n(\theta-\phi)),\ R<\rho, \end{cases} \tag{19}$$

$$M(s,x)=\begin{cases} M^I(s,x)=\displaystyle\sum_{n=0}^{\infty}\frac{\varepsilon_n k^2\pi}{2}\left[-iJ_n'(kR)+Y_n'(kR)\right]J_n'(k\rho) \\ \qquad \cos(n(\theta-\phi)),\ R\ge\rho, \\ M^E(s,x)=\displaystyle\sum_{n=0}^{\infty}\frac{\varepsilon_n k^2\pi}{2}\left[-iJ_n'(k\rho)+Y_n'(k\rho)\right]J_n'(kR) \\ \qquad \cos(n(\theta-\phi)),\ R<\rho, \end{cases} \tag{20}$$

where J_n, Y_n, J_n' and Y_n' are the first-kind and second-kind Bessel functions of the n^{th} order and their derivatives, the superscripts of *I* and *E* denote the interior and exterior cases for the expressions of kernel, respectively, and ε_n is the Neumann factor.

$$\varepsilon_n=\begin{cases}1, & n=0\\ 2, & n=1,2,\ldots\infty\end{cases} \tag{21}$$

It is noted that the degenerate kernel of *T* and *L* expressions for $\rho = R$ is not given since it is not continuous across the boundary.

III. PROOF OF EXISTENCE FOR THE SPURIOUS EIGENSOLUTION OF THE ANNULAR MEMBRANE

In order to fully utilize the geometry of circular boundary, the potential *u* and its normal derivative *t* can be approximated by employing the Fourier series. Therefore, we obtain

$$u_1(s)=\sum_{n=0}^{\infty}(p_{1,n}\cos(n\theta)+q_{1,n}\sin(n\theta)),\quad s\in B_1, \tag{22}$$

$$u_2(s)=\sum_{n=0}^{\infty}(p_{2,n}\cos(n\theta)+q_{2,n}\sin(n\theta)),\quad s\in B_2, \tag{23}$$

$$t_1(s)=\sum_{n=0}^{\infty}(a_{1,n}\cos(n\theta)+b_{1,n}\sin(n\theta)),\quad s\in B_1, \tag{24}$$

$$t_2(s)=\sum_{n=0}^{\infty}(a_{2,n}\cos(n\theta)+b_{2,n}\sin(n\theta)),\quad s\in B_2, \tag{25}$$

where θ is the polar angle, $a_{i,n}$, $b_{i,n}$, $p_{i,n}$ and $q_{i,n}$ (i = 1, 2) are the Fourier coefficients on B_i (i = 1, 2). When the field point is located on the inner boundary B_1, substitution of (22)-(25) into the dual null-field integral equations yields.

$$\begin{aligned} 0=&-\int_{B_1}U(s_1,x_1)\sum_{n=0}^{\infty}\left(a_{1,n}\cos(n\theta)+b_{1,n}\sin(n\theta)\right)dB(s)\\ &-\int_{B_2}U(s_2,x_1)\sum_{n=0}^{\infty}\left(a_{2,n}\cos(n\theta)+b_{2,n}\sin(n\theta)\right)dB(s)\\ &+\int_{B_1}T(s_1,x_1)\sum_{n=0}^{\infty}\left(p_{1,n}\cos(n\theta)+q_{1,n}\sin(n\theta)\right)dB(s)\\ &+\int_{B_2}T(s_2,x_1)\sum_{n=0}^{\infty}\left(p_{2,n}\cos(n\theta)+q_{2,n}\sin(n\theta)\right)dB(s),\\ &x_1\in B_1 \end{aligned} \tag{26}$$

$$
\begin{aligned}
0 = &-\int_{B_1} L(s_1, x_1)\sum_{n=0}^{\infty}(a_{1,n}\cos n\boldsymbol{\theta} + b_{1,n}\sin n\boldsymbol{\theta})\, dB(s) \\
&-\int_{B_2} L(s_2, x_1)\sum_{n=0}^{\infty}\left(a_{2,n}\cos n\boldsymbol{\theta} + b_{2,n}\sin n\boldsymbol{\theta}\right) dB(s) \\
&+\int_{B_1} M(s_1, x_1)\sum_{n=0}^{\infty}\left(p_{1,n}\cos n\boldsymbol{\theta} + q_{1,n}\sin n\boldsymbol{\theta}\right) dB(s) \\
&+\int_{B_2} M(s_2, x_1)\sum_{n=0}^{\infty}\left(p_{2,n}\cos n\boldsymbol{\theta} + q_{2,n}\sin n\boldsymbol{\theta}\right) dB(s), \\
&x_1 \in B_1
\end{aligned} \tag{27}
$$

When the field point is located on the outer boundary B_2, substitution of (22)-(25) into the dual null-field integral equation yields.

$$
\begin{aligned}
0 = &-\int_{B_1} U(s_1, x_2)\sum_{n=0}^{\infty}\left(a_{1,n}\cos(n\theta) + b_{1,n}\sin(n\theta)\right) dB(s) \\
&-\int_{B_2} U(s_2, x_2)\sum_{n=0}^{\infty}\left(a_{2,n}\cos(n\theta) + b_{2,n}\sin(n\theta)\right) dB(s) \\
&+\int_{B_1} T(s_1, x_2)\sum_{n=0}^{\infty}\left(p_{1,n}\cos(n\theta) + q_{1,n}\sin(n\theta)\right) dB(s) \\
&+\int_{B_2} T(s_2, x_2)\sum_{n=0}^{\infty}\left(p_{2,n}\cos(n\theta) + q_{2,n}\sin(n\theta)\right) dB(s), \\
&x_2 \in B_2
\end{aligned} \tag{28}
$$

$$
\begin{aligned}
0 = &-\int_{B_1} L(s_1, x_2)\sum_{n=0}^{\infty}(a_{1,n}\cos n\boldsymbol{\theta} + b_{1,n}\sin n\boldsymbol{\theta})\, dB(s) \\
&-\int_{B_2} L(s_2, x_2)\sum_{n=0}^{\infty}\left(a_{2,n}\cos n\boldsymbol{\theta} + b_{2,n}\sin n\boldsymbol{\theta}\right) dB(s) \\
&+\int_{B_1} M(s_1, x_2)\sum_{n=0}^{\infty}\left(p_{1,n}\cos n\boldsymbol{\theta} + q_{1,n}\sin n\boldsymbol{\theta}\right) dB(s) \\
&+\int_{B_2} M(s_2, x_2)\sum_{n=0}^{\infty}\left(p_{2,n}\cos n\boldsymbol{\theta} + q_{2,n}\sin n\boldsymbol{\theta}\right) dB(s), \\
&x_2 \in B_2
\end{aligned} \tag{29}
$$

For the Dirichlet problem, an annular case with radii a and b is shown in Fig. 1. Equation (26) is reduced to

$$
\begin{aligned}
&\int_{B_1} U^I(s,x)t(s)dB(s) + \int_{B_2} U^I(s,x)t(s)dB(s) \\
&= \sum_{n=0}^{\infty}\frac{\varepsilon_n}{2}\pi^2 aJ_n(ka)[Y_n(ka) - iJ_n(ka)] \\
&\quad (a_{1,n}\cos n\theta) + b_{1,n}\sin n\theta) \\
&+ \sum_{n=0}^{\infty}\frac{\varepsilon_n}{2}\pi^2 bJ_n(ka)[Y_n(kb) - iJ_n(kb)] \\
&\quad (a_{2,n}\cos n\theta) + b_{2,n}\sin n\theta) \\
&= 0, \quad x \in B_1
\end{aligned} \tag{30}
$$

According to (30), the Fourier coefficients $a_{1,n}$, $b_{1,n}$, $a_{2,n}$ and $b_{2,n}$ satisfy the relations:

$$
a_{2,n} = -\frac{aJ_n(ka)[Y_n(ka) - iJ_n(ka)]}{bJ_n(ka)[Y_n(kb) - iJ_n(kb)]}a_{1,n}, \quad n = 0, 1, 2, \cdots, \tag{31}
$$

$$
b_{2,n} = -\frac{aJ_n(ka)[Y_n(ka) - iJ_n(ka)]}{bJ_n(ka)[Y_n(kb) - iJ_n(kb)]}b_{1,n}, \quad n = 0, 1, 2, \cdots, \tag{32}
$$

and (28) is reduced to

$$
\begin{aligned}
&\int_{B_1} U^E(s,x)t(s)dB(s) + \int_{B_2} U^E(s,x)t(s)dB(s) \\
&= \sum_{n=0}^{\infty}\frac{\varepsilon_n}{2}\pi^2 aJ_n(ka)[Y_n(kb) - iJ_n(kb)] \\
&\quad (a_{1,n}\cos n\theta) + b_{1,n}\sin n\theta) \\
&+ \sum_{n=0}^{\infty}\frac{\varepsilon_n}{2}\pi^2 bJ_n(kb)[Y_n(kb) - iJ_n(kb)] \\
&\quad (a_{2,n}\cos n\theta) + b_{2,n}\sin n\theta) \\
&= 0, \quad x \in B_2
\end{aligned} \tag{33}
$$

Similarly, we obtain the relations among $a_{1,n}$, $b_{1,n}$, $a_{2,n}$ and $b_{2,n}$ as follows:

$$
a_{2,n} = -\frac{aJ_n(ka)[Y_n(kb) - iJ_n(kb)]}{bJ(kb)[Y_n(kb) - iJ_n(kb)]}a_{1,n}, \quad n = 0, 1, 2, \cdots, \tag{34}
$$

$$
b_{2,n} = -\frac{aJ_n(ka)[Y_n(kb) - iJ_n(kb)]}{bJ(kb)[Y_n(kb) - iJ_n(kb)]}b_{1,n}, \quad n = 0, 1, 2, \cdots, \tag{35}
$$

To seek the nontrivial data for the Fourier coefficient of $a_{1,n}$, $b_{1,n}$, $a_{2,n}$ and $b_{2,n}$ we obtain the eigenequation:

$$
J_n(ka)[J_n(kb)Y_n(ka) - J_n(ka)Y_n(kb)] = 0, \tag{36}
$$

The first term ($J_n(k_a) = 0$) in (36) is the spurious eigenequation, it is also the true eigenequation of circular membrane with the fixed boundary condition. The latter part in the bracket is the true eigenequation,

$$
J_n(kb)Y_n(ka) - J_n(ka)Y_n(kb) = 0. \tag{37}
$$

For the Neumann problem, Eq. (26) is reduced to

$$
\begin{aligned}
&\int_{B_1} T^I(s,x)u(s)dB(s) + \int_{B_2} T^I(s,x)u(s)dB(s) \\
&= \sum_{n=0}^{\infty}\frac{\varepsilon_n}{2}\pi^2 aJ_n(ka)[Y_n'(ka) - iJ_n'(ka)] \\
&\quad (p_{1,n}\cos n\theta) + q_{1,n}\sin n\theta) \\
&+ \sum_{n=0}^{\infty}\frac{\varepsilon_n}{2}\pi^2 bJ_n(ka)[Y_n'(kb) - iJ_n'(kb)] \\
&\quad (p_{2,n}\cos n\theta) + q_{2,n}\sin n\theta) \\
&= 0, \quad x \in B_1
\end{aligned} \tag{38}
$$

Table 1. Eigensolutions and boundary modes for the annular membrane subject to different boundary conditions.

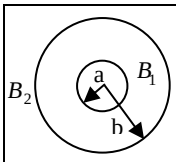 BC / Solution		Fixed-fixed $u_1 = u_2 = 0$	Free-fixed $t_1 = u_2 = 0$	Fixed-free $u_1 = t_2 = 0$	Free-free $t_1 = t_2 = 0$
UT formulation	True eigenequation	$J_n(kb)Y_n(ka) - J_n(ka)Y_n(kb) = 0$	$J_n(kb)Y_n'(ka) - J_n'(ka)Y_n(kb) = 0$	$J_n'(kb)Y_n(ka) - J_n(ka)Y_n'(kb) = 0$	$J_n'(kb)Y_n'(ka) - J_n'(ka)Y_n'(kb) = 0$
	Spurious eigenequation	$J_n(ka) = 0$	$J_n(ka) = 0$	$J_n(ka) = 0$	$J_n(ka) = 0$
	Inner boundary mode	$a_{1,n}^2 + b_{1,n}^2 \neq 0$	$p_{1,n}^2 + q_{1,n}^2 \neq 0$	$a_{1,n}^2 + b_{1,n}^2 \neq 0$	$p_{1,n}^2 + q_{1,n}^2 \neq 0$
	Outer boundary mode	$a_{2,n} = \frac{aJ_n(ka)}{bJ_n(kb)} a_{1,n}$	$a_{2,n} = \frac{aJ_n'(ka)}{bJ_n(kb)} p_{1,n}$	$p_{2,n} = \frac{aJ_n(ka)}{bJ_n'(kb)} a_{1,n}$	$p_{2,n} = \frac{aJ_n'(ka)}{bJ_n'(kb)} p_{1,n}$
LM formulation	True eigenequation	$J_n(kb)Y_n(ka) - J_n(ka)Y_n(kb) = 0$	$J_n(kb)Y_n'(ka) - J_n'(ka)Y_n(kb) = 0$	$J_n'(kb)Y_n(ka) - J_n(ka)Y_n'(kb) = 0$	$J_n'(kb)Y_n'(ka) - J_n'(ka)Y_n'(kb) = 0$
	Spurious eigenequation	$J_n'(ka) = 0$	$J_n'(ka) = 0$	$J_n'(ka) = 0$	$J_n'(ka) = 0$
	Inner boundary mode	$a_{1,n}^2 + b_{1,n}^2 \neq 0$	$p_{1,n}^2 + q_{1,n}^2 \neq 0$	$a_{1,n}^2 + b_{1,n}^2 \neq 0$	$p_{1,n}^2 + q_{1,n}^2 \neq 0$
	Outer boundary mode	$a_{2,n} = \frac{aJ_n(ka)}{bJ_n(kb)} a_{1,n}$	$a_{2,n} = \frac{aJ_n'(ka)}{bJ_n(kb)} p_{1,n}$	$p_{2,n} = \frac{aJ_n(ka)}{bJ_n'(kb)} a_{1,n}$	$p_{2,n} = \frac{aJ_n'(ka)}{bJ_n'(kb)} p_{1,n}$

According to (37), the Fourier coefficients, $a_{1,n}$, $b_{1,n}$, $a_{2,n}$ and $b_{2,n}$ satisfy the relations:

$$p_{2,n} = -\frac{aJ_n(ka)[Y_n'(ka) - iJ_n'(ka)]}{bJ_n(ka)[Y_n'(kb) - iJ_n'(kb)]} p_{1,n}, \quad n = 0, 1, 2, \cdots, \quad (39)$$

$$q_{2,n} = -\frac{aJ_n(ka)[Y_n'(ka) - iJ_n'(ka)]}{bJ_n(ka)[Y_n'(kb) - iJ_n'(kb)]} q_{1,n}, \quad n = 0, 1, 2, \cdots, \quad (40)$$

Equation (28) is reduced to

$$\begin{aligned} &\int_{B_1} T^E(s,x)u(s)dB(s) + \int_{B_2} T^E(s,x)u(s)dB(s) \\ &= \sum_{n=0}^{\infty} \frac{\varepsilon_n}{2} \pi^2 aJ_n'(ka)[Y_n(kb) - iJ_n(kb)] \\ &\quad (p_{1,n}\cos n\theta) + q_{1,n}\sin n\theta) \\ &+ \sum_{n=0}^{\infty} \frac{\varepsilon_n}{2} \pi^2 bJ_n'(kb)[Y_n(kb) - iJ_n(kb)] \\ &\quad (p_{2,n}\cos n\theta) + q_{2,n}\sin n\theta) \\ &= 0, \quad x \in B_2 \end{aligned} \quad (41)$$

Similarly we obtain the relations among $a_{1,n}$, $b_{1,n}$, $a_{2,n}$ and $b_{2,n}$ as follows:

$$p_{2,n} = -\frac{aJ'_n(ka)[Y_n(kb) - iJ_n(kb)]}{bJ_n'(kb)[Y_n(kb) - iJ_n(kb)]} p_{1,n}, \quad n = 0, 1, 2, \cdots, \quad (42)$$

$$q_{2,n} = -\frac{aJ'_n(ka)[Y_n(kb) - iJ_n(kb)]}{bJ_n'(kb)[Y_n(kb) - iJ_n(kb)]} q_{1,n}, \quad n = 0, 1, 2, \cdots, \quad (43)$$

To seek the nontrivial data for the Fourier coefficient of $a_{1,n}$, $b_{1,n}$, $a_{2,n}$ and $b_{2,n}$, we obtain the eigenequation:

$$J_n(ka)[J_n'(kb)Y_n'(ka) - J_n'(ka)Y_n'(kb)] = 0, \quad (44)$$

The first term ($J_n(ka) = 0$) is the spurious eigenequation, which is also the true eigenequation of circular membrane with the fixed boundary condition. The latter part in the bracket is the true eigenequation,

$$J_n'(kb)Y_n'(ka) - J_n'(ka)Y_n'(kb) = 0. \quad (45)$$

The spurious eigenequation and true eigenequation of the annular membrane subject to various boundary conditions are listed in Table 1. It is interesting to find that spurious eigenvalue of *UT* singular method results in trivial outer boundary modes for the fixed-fixed case. Besides, spurious eigenvalue of *LM* hypersingular method results in the trivial outer boundary modes of free-free case.

IV. PROOF OF THE EXISTENCE FOR THE SPURIOUS EIGENSOLUTION OF THE ECCENTRIC MEMBRANE

1. Dirichlet Problem by Using the Singular (*UT*) Formulation

In order to prove that the spurious eigensolution of eccentric membrane subject to the Dirichlet boundary condition satisfies the BIE by collocating the inner and outer boundary points, we first derive the true eigensolution of a circular membrane.

Now, we consider the circular fixed membrane with a radius a in the continuous system. By using the null-field integral equation and collocating the point on the boundary for the *UT* singular formulation, we obtain the eigenequation,

$$[-iJ_n(ka)+Y_n(ka)]J_n(ka)=0. \tag{46}$$

The true eigenequation is

$$J_n(ka)=0, \tag{47}$$

and the corresponding true eigenmode are

$$\begin{Bmatrix} a_n \\ b_n \end{Bmatrix}, \tag{48}$$

where a_n and b_n are the Fourier coefficients on the circular boundary and $a_n^2+b_n^2\neq 0$. By collocating the point in the complementary domain ($x^c \in D^c$) as shown in Fig. 2, the null-field equation yields

$$0=\int_{B_1} U^E(s,x^c)t(s)dB(s), \quad x^c\in D^c \tag{49}$$

where $t(s)=\sum_{n=0}^{\infty}\left(a_n\cos(n\theta)+b_n\sin(n\theta)\right)$. For any point $x^c \in D^c$, we obtain the null-field response for x^c at the location a^c as shown below

$$[-iJ_n(ka^c)+Y_n(ka^c)]J_n(ka)(a_n\cos n\theta+b_n\sin n\theta)=0,$$

$$n = 0, 1, 2, 3, \ldots, \tag{50}$$

since k satisfies $J_n(ka) = 0$.

Secondly, we consider the eccentric case subject to the fixed-fixed boundary condition as shown in Fig. 3. To satisfy (26) and (28) of BIE model, we need to seek a nontrivial boundary mode for ($a_{1,n}$, $b_{1,n}$, $a_{2,n}$, $b_{2,n}$). By selecting a nontrivial boundary mode for the $J_n(ka) = 0$, computer-assisted experiment inspires us to choose

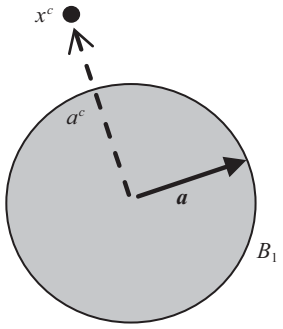

Fig. 2. A circular fixed membrane of collocating point (a^c).

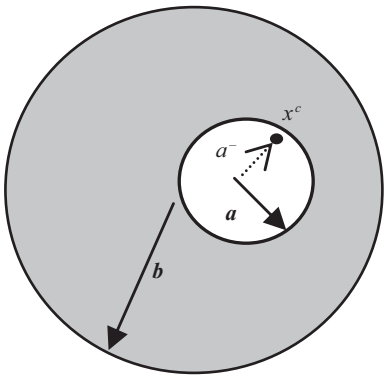

Fig. 3. An eccentric case of collocating point (a^-).

$$\begin{Bmatrix} a_{1,n} \\ b_{1,n} \\ a_{2,n} \\ b_{2,n} \end{Bmatrix} = \begin{Bmatrix} a_n \\ b_n \\ 0 \\ 0 \end{Bmatrix}. \tag{51}$$

Equation (26) is satisfied since $U^I(s,a^-) = U^E(s,a^+)$ in (17). It is found that the nontrivial boundary mode of (51) in case of $J_n(ka) = 0$, also satisfies (28) due to (17). This indicates that $J_n(ka) = 0$ of (47) and the nontrivial boundary mode of (51) in conjunction with the trivial outer boundary data satisfy (26) and (28). In other words, the solution space to satisfy (26) and (28) of the singular formulation only seems bigger. To make the BIEM model well-posed without spurious solutions, dual formulation is necessary. Spurious eigenvalue with the trivial outer boundary mode happens to be the true eigenvalue of domain bounded by the inner boundary.

2. Neumann Problem by Using the Hypersingular (LM) Formulation

Similarly, we consider the circular free membrane with a radius a in the continuous system. By using the null-field integral equation and collocating the point on the boundary for the hypersingular (*LM*) formulation, we obtain the eigenequation,

$$[-iJ_n'(ka)+Y_n'(ka)]J_n'(ka)=0. \tag{52}$$

The true eigenequation is

$$J_n'(ka)=0, \tag{53}$$

and the corresponding true eigenmode are

$$\begin{Bmatrix} p_n \\ q_n \end{Bmatrix}, \tag{54}$$

where p_n and q_n are the Fourier coefficients on the circular boundary and $p_n^2+q_n^2\neq 0$. By collocating the point in the complementary domain ($x^c \in D^c$) as shown in Fig. 2, the null-field equation yields

$$0=\int_{B_1} M^E(s,x^c)u(s)dB(s), \quad x^c\in D^c \tag{55}$$

where $u(s)=\sum_{n=0}^{\infty}(p_n\cos(n\theta)+q_n\sin(n\theta))$. For any point $x^c \in D^c$, we obtain the null-field response for x^c as shown below

$$[-iJ_n'(ka^c)+Y_n'(ka^c)]J_n'(ka)(p_n\cos n\theta+q_n\sin n\theta)=0,$$

$$n = 0, 1, 2, 3, \ldots, \tag{56}$$

since k satisfies $J_n'(ka)=0$.

Secondly, we consider the eccentric case subject to the free-free boundary condition as shown in Fig. 3. To satisfy (27) and (29) of the BIE model, we need to seek a nontrivial boundary mode for ($p_{1,n}$, $q_{1,n}$, $p_{2,n}$, $q_{2,n}$). By selecting a nontrivial boundary mode for the $J_n'(ka)=0$, computer-assisted experiment inspires us to choose

$$\begin{Bmatrix} p_{1,n} \\ q_{1,n} \\ p_{2,n} \\ q_{2,n} \end{Bmatrix} = \begin{Bmatrix} p_n \\ q_n \\ 0 \\ 0 \end{Bmatrix}. \tag{57}$$

Equation (27) is satisfied since $M^I(s,a^-)=M^E(s,a^+)$ in (21). It is found that nontrivial boundary mode of (57) in case of $J_n'(ka)=0$, also satisfies (29) due to (21). This indicates that $J_n'(ka)=0$ of (53) and the nontrivial boundary mode of (57) satisfy (27) and (29). Spurious eigenvalue in companion with the trivial outer boundary mode happens to be the true eigenvalue of domain bounded by the inner boundary.

V. SVD TECHNIQUE FOR EXTRACTING OUT TRUE AND SPURIOUS EIGENVALUES BY USING UPDATING TERMS AND UPDATING DOCUMENT

1. Method to Extract the True Eigensolutions

The matrix [**A**] with a dimension M by N by using singular value decomposition technique can be decomposed into a product of the unitary matrix [**Φ**] (M by M), the diagonal matrix [**Σ**] (M by N) with positive or zero elements, and the unitary matrix [**Ψ**] (N by N)

$$[\mathbf{A}]_{M\times N}=[\mathbf{\Phi}]_{M\times M}[\mathbf{\Sigma}]_{M\times N}[\mathbf{\Psi}]^H_{N\times N}, \tag{58}$$

where the superscript "H" is the Hermitian, [**Φ**] and [**Ψ**] are both unitary that their column vectors which satisfy

$$\underset{\sim}{\phi}_i\cdot\underset{\sim}{\phi}_j^H=\delta_{ij}, \tag{59}$$

$$\underset{\sim}{\psi}_i\cdot\underset{\sim}{\psi}_j^H=\delta_{ij}, \tag{60}$$

in which $[\mathbf{\Phi}]^H[\mathbf{\Phi}]=[\mathbf{I}]_{M\times M}$ and $[\mathbf{\Psi}]^H[\mathbf{\Psi}]=[\mathbf{I}]_{N\times N}$. For the eigenproblem, we can obtain a nontrivial solution for the homogeneous system from a column vector $\{\boldsymbol{\psi}_i\}$ of [**Ψ**] when the singular value (σ_i) is zero. For the direct BEM, we have

Singular formulation (UT method)

$$[\mathbf{T}^E]\{u\}=[\mathbf{U}^E]\{t\}=\{0\}, \tag{61}$$

Hypersingular formulation (LM method)

$$[\mathbf{M}^E]\{u\}=[\mathbf{L}^E]\{t\}=\{0\}, \tag{62}$$

where $\{u\}$ and $\{t\}$ are the boundary excitations.

For the Dirichlet problem, Eqs. (61) and (62) can be combined to have

$$\begin{bmatrix} \mathbf{U}^E \\ \mathbf{L}^E \end{bmatrix}\{t\}=\{0\}. \tag{63}$$

By using the SVD technique, the two submatrices in (61) and (62) can be combined to have

$$[\mathbf{U}^E]=[\mathbf{\Phi}^{(U)}][\mathbf{\Sigma}^{(U)}][\mathbf{\Psi}^{(U)}]^H \text{ or}$$

$$[\mathbf{U}^E]=\sum_j\{\boldsymbol{\sigma}_j^{(U)}\}\{\boldsymbol{\phi}_j^{(U)}\}\{\boldsymbol{\psi}_j^{(U)}\}^H, \tag{64}$$

$$\left[\mathbf{L}^{e}\right]=\left[\mathbf{\Phi}^{(L)}\right]\left[\mathbf{\Sigma}^{(L)}\right]\left[\mathbf{\Psi}^{(L)}\right]^{H} \text{ or}$$

$$\left[\mathbf{L}^{E}\right]=\sum_{j}\left\{\boldsymbol{\sigma}_{j}^{(L)}\right\}\left\{\boldsymbol{\phi}_{j}^{(L)}\right\}\left\{\boldsymbol{\psi}_{j}^{(L)}\right\}^{H}, \tag{65}$$

where the superscripts, (*U*) and (*L*), denote the corresponding matrices. For the linear algebraic system, $\{t\}$ is a column vector of $\{\boldsymbol{\psi}_i\}$ in the matrix $[\mathbf{\Psi}]$ corresponding to the zero singular value ($\sigma_i = 0$). By setting $\{t\}$ as a vector of $\{\boldsymbol{\psi}_i\}$, in the right unitary matrix for the true eigenvalue k_t, Eq. (63) reduces to

$$\left[\mathbf{U}^{E}\left(k_{T}\right)\right]\{\boldsymbol{\psi}_{i}\}=\{0\}, \tag{66}$$

$$\left[\mathbf{L}\left(k_{T}\right)\right]\{\boldsymbol{\psi}_{i}\}=\{0\}. \tag{67}$$

According to (64)-(67), we have

$$\boldsymbol{\sigma}_{j}^{(U)}\left\{\boldsymbol{\phi}_{j}^{(U)}\right\}=\{0\}, \tag{68}$$

$$\boldsymbol{\sigma}_{j}^{(L)}\left\{\boldsymbol{\phi}_{j}^{(L)}\right\}=\{0\}. \tag{69}$$

We can easily extract out the true eigenvalues, $\boldsymbol{\sigma}_{j}^{(U)} = \boldsymbol{\sigma}_{j}^{(L)} = \{0\}$, since there exists the same eigensolusion ($\{t\} = \{\boldsymbol{\psi}_i\}$) for the Dirichlet problem using (63) or (66) and (67). In a similar way, Eqs. (61) and (62) can be combined to have

$$\begin{bmatrix}\mathbf{T}^{E}\left(k_{T}\right)\\ \mathbf{M}^{E}\left(k_{T}\right)\end{bmatrix}\{u\}=\{0\}, \tag{70}$$

for the Neumann problem. We can easily extract out the true eigenvalues for the Neumann problem with respect to the j^{th} zero singular values of $\boldsymbol{\sigma}_{j}^{(T)}=\boldsymbol{\sigma}_{j}^{(M)}=\{0\}$.

2. Method to Filter Out the Spurious Eugensolutions

By employing the LM formulation in the direct BEM, we have

$$\left[\mathbf{M}^{E}\right]\{u\}=\left[\mathbf{L}^{E}\right]\{t\}=\{p\}. \tag{71}$$

Since the spurious eigenvalue k_s is embedded in both the Dirichlet and Neumann problems, we have

$$\{p\}^{H}\{\boldsymbol{\phi}_{i}\}=\{0\}, \tag{72}$$

where $\{\boldsymbol{\phi}_i\}$ satisfies

$$\left[\mathbf{L}^{E}\left(k_{S}\right)\right]^{H}\{\boldsymbol{\phi}_{i}\}=\{0\}, \text{ for the Dirichlet problem} \tag{73}$$

$$\left[\mathbf{M}^{E}\left(k_{S}\right)\right]^{H}\{\boldsymbol{\phi}_{i}\}=\{0\}, \text{ for the Neumann problem} \tag{74}$$

according to the Fredholm alternative theorem. By substituting (71) into (73) and (74), we have

$$\{u\}^{H}\left[\mathbf{M}^{E}\left(k_{s}\right)\right]^{H}\{\boldsymbol{\phi}_{i}\}=\{0\}, \text{ for the Dirichlet problem} \tag{75}$$

$$\{t\}^{H}\left[\mathbf{L}^{E}\left(k_{s}\right)\right]^{H}\{\boldsymbol{\phi}_{i}\}=\{0\}, \text{ for the Neumann problem} \tag{76}$$

Since $\{u\}$ and $\{t\}$ can be arbitrary boundary excitation for the Dirchlet problem and Neumann problem, respectively, this yields

$$\left[\mathbf{M}^{E}\left(k_{s}\right)\right]^{H}\{\boldsymbol{\phi}_{i}\}=\{0\}, \text{ for the Dirichelt problem} \tag{77}$$

$$\left[\mathbf{L}^{E}\left(k_{s}\right)\right]^{H}\{\boldsymbol{\phi}_{i}\}=\{0\}, \text{ for the Neumann problem} \tag{78}$$

By combining (73) and (74) with (77) and (78) for the Dirichlet problem, we have

$$\begin{bmatrix}\left[\mathbf{L}^{E}\right]^{H}\\ \left[\mathbf{M}^{E}\right]^{H}\end{bmatrix}\{\boldsymbol{\phi}_{i}\}=\{0\} \text{ or } \{\boldsymbol{\phi}_{i}\}^{H}\left[\left[\mathbf{L}^{E}\right]\ \left[\mathbf{M}^{E}\right]\right]=\{0\}. \tag{79}$$

It indicates that two matrices have the same spurious boundary mode $\{\boldsymbol{\phi}_i\}$ corresponding to the i^{th} zero singular values. By using the SVD technique, the two matrices in (79) ca be decomposed into

$$\left[\mathbf{L}^{E}\right]^{H}=\left[\mathbf{\Psi}^{(U)}\right]\left[\mathbf{\Sigma}^{(U)}\right]\left[\mathbf{\Phi}^{(U)}\right]^{H} \text{ or}$$

$$\left[\mathbf{L}_{\boldsymbol{\lambda}}^{E}\right]^{H}=\sum_{j}\boldsymbol{\sigma}_{j}^{(L)}\left\{\boldsymbol{\psi}_{j}^{(L)}\right\}\left\{\boldsymbol{\phi}_{j}^{(L)}\right\}^{H}, \tag{80}$$

$$\left[\mathbf{M}^{E}\right]^{H}=\left[\mathbf{\Psi}^{(M)}\right]\left[\mathbf{\Sigma}^{(M)}\right]\left[\mathbf{\Phi}^{(M)}\right]^{H} \text{ or}$$

$$\left[\mathbf{M}_{\boldsymbol{\lambda}}^{E}\right]^{H}=\sum_{j}\boldsymbol{\sigma}_{j}^{(L)}\left\{\boldsymbol{\psi}_{j}^{(L)}\right\}\left\{\boldsymbol{\phi}_{j}^{(L)}\right\}^{H}. \tag{81}$$

By substituting (80) and (81) into (75) and (76), we have

$$\boldsymbol{\sigma}_{j}^{(L)}\left\{\boldsymbol{\psi}_{j}^{(L)}\right\}=\{0\}, \tag{82}$$

$$\boldsymbol{\sigma}_{j}^{(M)}\left\{\boldsymbol{\psi}_{j}^{(M)}\right\}=\{0\}. \tag{83}$$

Table 2. (a) SVD structure of the four influence matrices for the Dirichlet and Neumann problems in the case of true eigenvalue. (b) SVD structure of the four influence matrices by using the *UT* singular formulation and *LM* hypersigular formulation in the case of spurious eigenvalue.

(a)

	Dirichlet problem ($k = k_T^D$)			
True eigenvalue k_T (k_T^D, k_T^N)	$[\Phi^U]\begin{bmatrix}0 & \\ & \ddots\end{bmatrix}\begin{bmatrix}\underset{\sim}{\varphi}_1^D \cdots\end{bmatrix}^H$ The same $\underset{\sim}{\varphi}_1$	$[\Phi^T][\Sigma^T][\Psi^T]^H$	$[\Phi^U][\Sigma^U][\Psi^U]^H$	$[\Phi^T]\begin{bmatrix}0 & \\ & \ddots\end{bmatrix}\begin{bmatrix}\underset{\sim}{\varphi}_1^N \cdots\end{bmatrix}^H$ The same $\underset{\sim}{\varphi}_1$
	$[\Phi^L]\begin{bmatrix}0 & \\ & \ddots\end{bmatrix}\begin{bmatrix}\underset{\sim}{\varphi}_1^D \cdots\end{bmatrix}^H$	$[\Phi^M][\Sigma^M][\Psi^M]^H$	$[\Phi^L][\Sigma^L][\Psi^L]^H$	$[\Phi^M]\begin{bmatrix}0 & \\ & \ddots\end{bmatrix}\begin{bmatrix}\underset{\sim}{\varphi}_1^N \cdots\end{bmatrix}^H$

U T / L M

where k_T^D and k_T^N devotes the true eigenvalues for the Dirichlet and Neumann problems.

(b)

	UT singular formulation ($k = k_S^{UT}$)		*LM* hypersingular formulation ($k = k_S^{LM}$)	
	Dirichlet	Neumann	Dirichlet	Neumann
Spurious eigenvalue k_S (k_S^{UT}, k_S^{LM})	$[\underset{\sim}{\phi}_1^{UT} \cdots]\begin{bmatrix}0 & \\ & \ddots\end{bmatrix}\begin{bmatrix}\underset{\sim}{\varphi}_1^D & \cdots \\ \{0\} & \end{bmatrix}^H$ The same $\underset{\sim}{\phi}_1$	$[\underset{\sim}{\phi}_1^{UT} \cdots]\begin{bmatrix}0 & \\ & \ddots\end{bmatrix}[\Psi^L]^H$	$[\underset{\sim}{\phi}_1^{LM} \cdots]\begin{bmatrix}0 & \\ & \ddots\end{bmatrix}[\Psi^L]^H$ The same $\underset{\sim}{\phi}_1$	$[\underset{\sim}{\phi}_1^{LM} \cdots]\begin{bmatrix}0 & \\ & \ddots\end{bmatrix}\begin{bmatrix}\underset{\sim}{\varphi}_1^N \cdots \\ \{0\} & \end{bmatrix}^H$
	U *T*		*L* *M*	

where k_S^{UT} and k_S^{LM} devotes the spurious eigenvalues by using *UT* singular and *LM* hypersigular formulation.

We can easily extract out the spurious eigenvalues since there exists the same spurious boundary mode $\{\underset{\sim}{\phi}_i\}$ corresponding the i^{th} zero singular value, $\sigma = \sigma_i^{(M)} = 0$. Similarly, the spurious eigenvalue parasitized in the UT formulation can be obtained by using SVD updating documents. To summarize the SVD structure for the four influence matrices, Tables 2(a) and 2(b) show that the spurious and true boundary modes are imbedded in the left and right unitary vectors, respectively. Besides, the nontrivial interior boundary mode and trivial outer boundary mode are given in Table 2(b).

VI. ILLUSTRATIVE EXAMPLES AND DISCUSSIONS

Case 1: An eccentric case subject to the Dirichlet boundary condition ($u_1 = u_2 = 0$) using the semi-analytical approach

An eccentric case with radii a and b ($a = 0.5\ m$, , $b = 2.0\ m$) is shown in Fig. 1. The eccentricity of eccentric membrane was changed from $e = 0.0$ to 1.0 m. Figure 4 shows the minimum singular value σ_1 versus k for the annular circular membrane by using the null-field BIE and using the truncated Fourier series ($M = 10$). Figure 5 shows the effect of the eccentricity e on the possible eigenvalues for the fixed membrane. It is interesting to find that the spurious eigenvalues of $k_s = 4.81$ and $k_s = 7.66$ occur no matter what the eccentricity e is. After checking the boundary eigenvectors from the bar chart, we find that the true eigenvectors for inner and outer boundaries are nontrivial as shown in Fig. 6 for the first true eigenvalue $k_t = 2.05$. For the spurious eigenvalues ($k_s = 4.81$, $k_s = 7.66$, $e = 0.0$), the outer boundary mode is trivial and only the nontrivial inner boundary mode is found as shown in Fig. 7, as theoretically proved. This phenomenon is also observed by using the BEM (40 elements) as shown in Fig. 8. Both figures indicate that null field BIEM use the generalized coordinate of Fouries series while BEM interpolates with nodal constant value. For the eccentricity of $e = 0.5\ m$, the similar result is

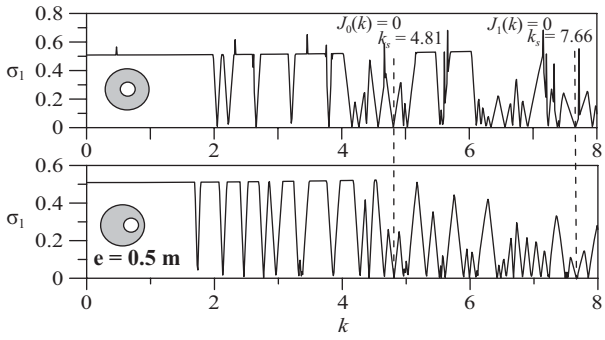

Fig. 4. The minimum singular value σ_1 versus k for the annular circular membrane subject to the Dirichlet boundary condition by using the *UT* null-field BIE (b = 2.0, a = 0.5).

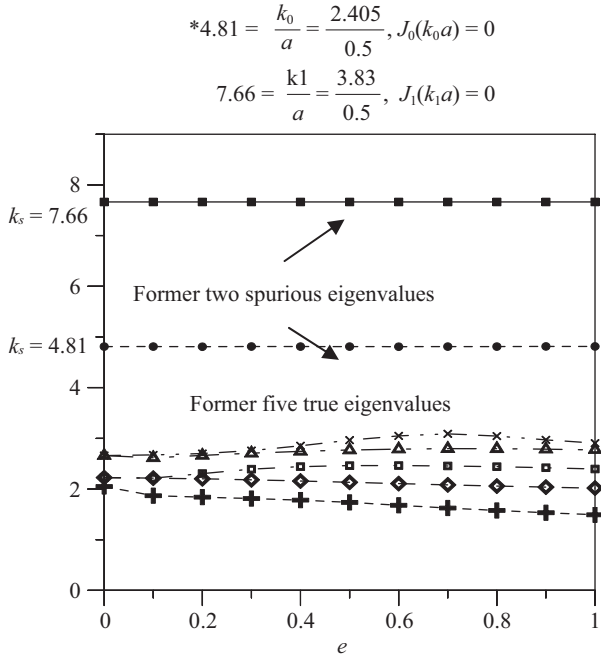

Fig. 5. Effect of the eccentricity e on the possible eigenvalues (true and spurious).

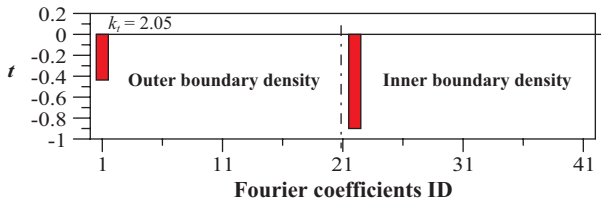

Fig. 6. Real part of Fourier coefficients for the first true boundary mode (k_t = 2.05, e = 0.0).

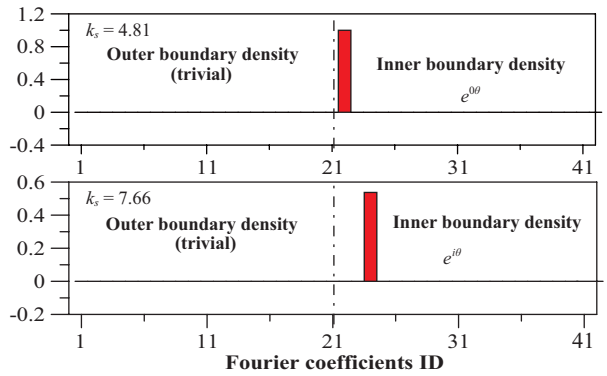

Fig. 7. Real part of Fourier coefficients for the first and second spurious boundary modes (k_s = 4.81, 7.66, e = 0.0).

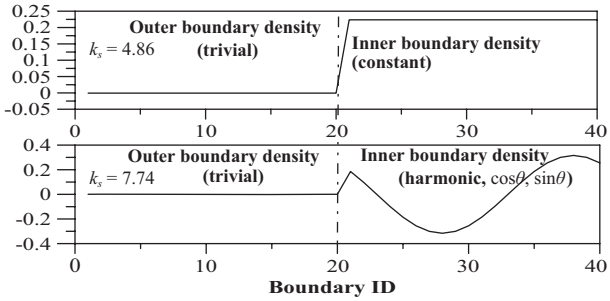

Fig. 8. Real part of the first spurious and second boundary modes by using BEM (k_s = 4.86, 7.74, e = 0.0).

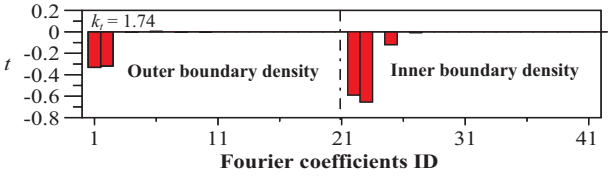

Fig. 9. Real part of Fourier coefficients for the first true boundary mode (k_t = 1.74, e = 0.5).

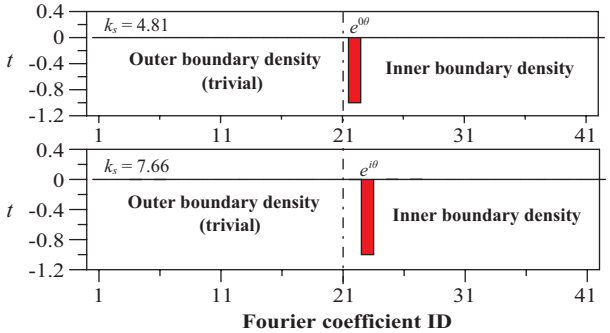

Fig. 10. Fourier coefficients for the first and second spurious boundary modes by using the *UT* null-field BIE (k_s = 4.81, 7.76, e = 0.5).

found as shown in Figs. 9-11. All the numerical results agree well with our theoretical prediction in the *UT* formulation. It is interesting to point out that the nontrivial inner boundary mode of eccentric case agree well with that of circular membrane as theoretically proved. For the null-field BIEM using Fourier series, we obtain only nonzero components of $a_{1,0}$ ($a_{1,1}$ or $b_{1,1}$) for the $J_0(ka)$ ($J_1(ka)$) case in Fig. 7. When the boundary density is interpolated by using constant elements of BEM, constant and simple harmonics (cosθ or sinθ) distribution for the inner boundary mode are found as shown in Fig. 8.

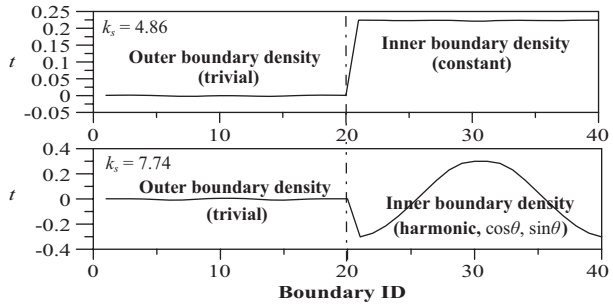

Fig. 11. The first and second spurious boundary modes by using BEM (40 elements, k_s = 4.86, 7.74, e = 0.5).

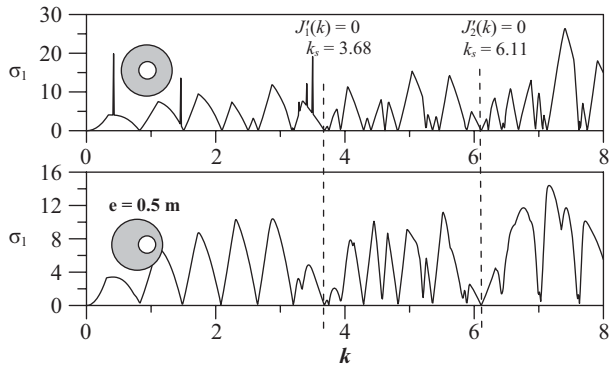

Fig. 12. The minimum singular value σ_1 versus k for the annular circular membrane subject to the Neumann boundary condition by using the *LM* null-field BIE (b = 2.0, a = 0.5).

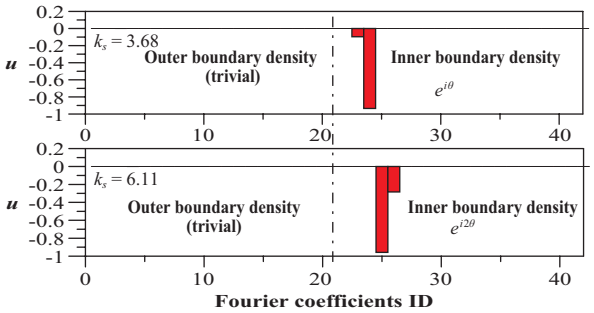

Fig. 13. Real part of Fourier coefficients for the first and second spurious boundary modes by using null-field BIEM (k_s = 3.68, 6.11, e = 0.0).

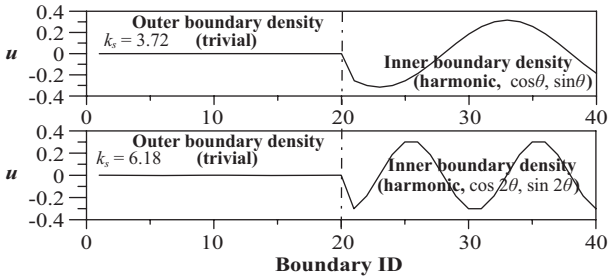

Fig. 14. Real part of the first and second spurious boundary modes by using BEM (k_s = 3.72, 6.18, e = 0.0).

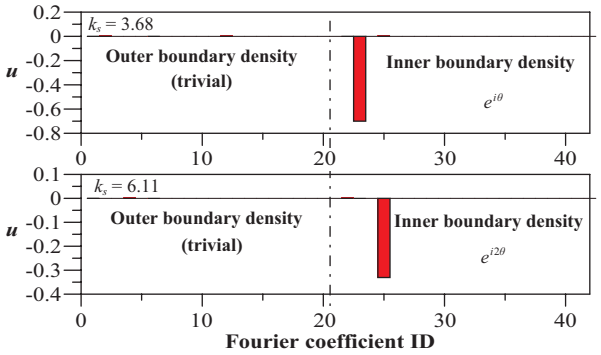

Fig. 15. Fourier coefficients for the first and second spurious boundary modes by using null-field BIEM (k_s = 3.68, 6.11, e = 0.5).

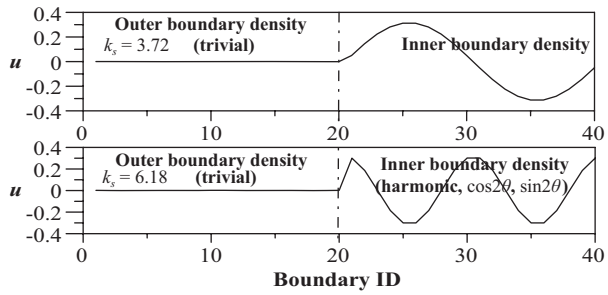

Fig. 16. Real part of the first and second spurious boundary modes by using BEM (k_s = 3.72, 6.18, e = 0.0).

Case 2: An eccentric case subject to the Neumann boundary condition ($t_1 = t_2 = 0$) using the semi-analytical approach

An eccentric case with radii a and b (a = 0.5 m, b = 2.0 m) is shown in Fig. 1. Figure 12 shows the minimum singular value σ_1 versus k for the annular circular membrane by using the null-field BIE, and using the truncated Fourier series (M = 10). It is found that the spurious eigenvalues of k_s = 3.68 and k_s = 6.11 occur on both cases of e = 0.0 and 0.5. For the spurious eigenvalue (k_s = 3.68, k_s = 6.11, e = 0.0), the outer boundary mode is trivial and only the nontrivial inner boundary mode is found as shown in Fig. 13. This phenomenon is also observed by using the BEM (40 elements) as shown in Fig. 14. For the eccentricity of e = 0.5 m, the similar result is found as shown in Figs. 15-16. All the numerical results agree well with our theoretical prediction. It is interesting to point out that the nontrivial inner boundary mode of eccentric case agree well with that of the circular membrane as theoretically proved in the *LM* hypersingular formulation.

Case 3: A square membrane with a circular hole by using BEM

A square (1 m × 1 m) membrane with a circular hole (b = 0.5 m) subjected to the Dirichlet boundary condition is shown in Fig. 17. Forty elements in the BEM mesh were adopted. Figure 18 shows the minimum singular value σ_1 versus k for

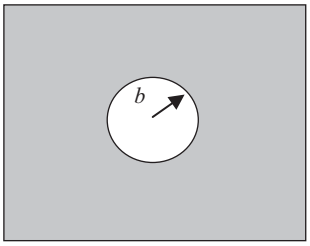

Case 3:
Rectangle = 1*m* × 1*m*
Circle: *b* = 0.5 *m*
Boundary condition:
Inner circle: *u* = 0
Outer rectangle: *u* = 0

Fig. 17. A rectangle membrane with one circular hole of radius 0.5 *m*.

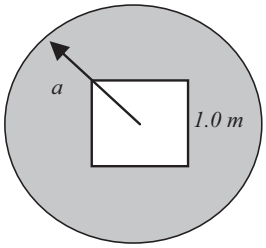

Case 4:
Square = 1 *m* × 1 *m*
Circle: *a* = 1.0 *m*
Boundary condition:
Inner square: *u* = 0
Outer circle: *u* = 0

Fig. 20. A circular membrane with one square hole.

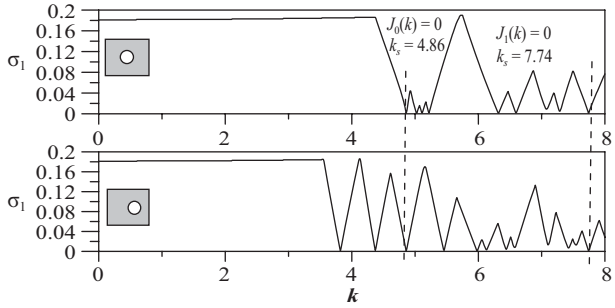

Fig. 18. The minimum singular value σ_1 versus *k* for the rectangle membrane with a circular hole by using BEM.

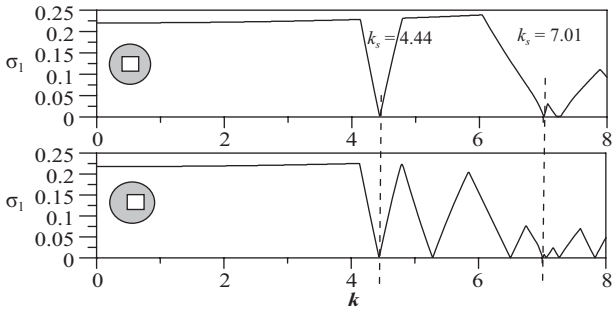

Fig. 21. The minimum singular value σ_1 versus *k* for the circular membrane with a square hole by using BEM.

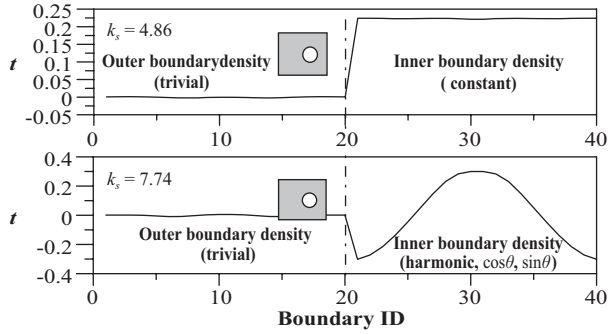

Fig. 19. The first and second spurious boundary modes by using BEM (40 elements, k_s = 4.86, 7.74, *e* = 0.5).

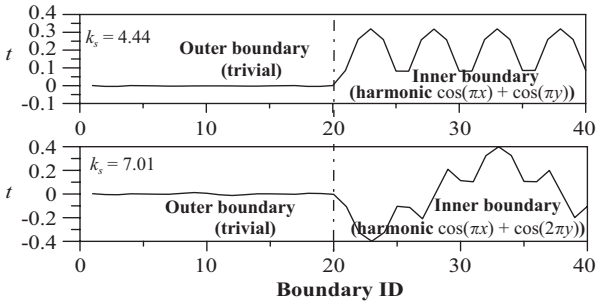

Fig. 22. The first and second spurious boundary modes by using BEM (40 elements, k_s = 4.44, 7.01, *e* = 0.2).

the Dirichlet problem by using BEM. It is found that the same spurious eigenvalues appeared at the k_s = 4.86 and 7.74, as shown in case 1 due to the same inner boundary. Figure 19 shows the first and second spurious boundary modes by using BEM (k_s = 4.86, 7.74, *e* = 0.5). The constant and simple harmonic (cosθ or sinθ) distribution for the nontrivial inner boundary mode are found for $J_0(ka) = 0$ and $J_1(ka) = 0$, respectively. As predicted, the outer boundary mode is trivial. No matter what the shape of the outer boundary is, the spurious eigenvalue always depends on the inner boundary.

Case 4: A circular membrane with a square hole by using BEM

A circular (*a* = 1.0 *m*) membrane with a square (1 *m* × 1 *m*) hole subjected to the Dirichlet boundary condition is shown in Fig. 20. Forty elements in the BEM mesh were adopted. Figure 21 shows the minimum singular value σ_1 versus *k* for the Dirichlet problem by using BEM. It is found that the same spurious eigenvalues appeared at the k_s = 4.44 and 7.01 (analytical solution is $k_{mn} = \pi\sqrt{\left(\frac{m}{b}\right)^2 + \left(\frac{n}{b}\right)^2}$, *m*, *n* = 0, 1, 2, …), due to the inner square boundary. Figure 22 shows the first and second spurious boundary modes by using BEM (k_s = 4.44, 7.01, *e* = 0.2). The simple harmonic (cosine function) for the nontrivial inner boundary mode are found to be $u_{11}(x, y) = \cos(\pi x)\cos(\pi y)$ and $u_{12}(x, y) = \cos(\pi x)\cos(2\pi y)$, respectively. No matter what the shape of the outer boundary is, the spurious eigenvalue only depends on the inner boundary.

VII. CONCLUDING REMARKS

Spurious eigenvalues for the doubly-connected membrane were studied analytically and numerically. Computer assisted proof for the existence of spurious eigenvalue in conjunction with the trivial outer boundary density was also done. Four

examples were demonstrated to see how the spurious eigenvalue occurs. The trivial outer boundary densities were found in case of spurious eigenvalues which is found to be the true eigenvalue for the domain bounded by the inner boundary. The contribution of the work is to show the existence of spurious eigenvalue occur in the doubly-connected problems in an analytical manner by using the degenerate kernels and the Fourier series. It can be easily extended to the problem containing multiple circles and arbitrarily shaped membrane.

ACKNOWLEDGMENTS

Financial support from the National Kaohsiung Marine University under Grant No. 97A018 is gratefully acknowledged.

REFERENCES

1. Burton, A. J. and Miller, G. F., "The application of integral equation methods to numerical solution of some exterior boundary value problems," *Proceedings of the Royal Society of London. Series A*, Vol. 323, pp. 201-210 (1971).
2. Chen, J. T., Chen, I. L., and Chen, K. H., "Treatment of rank deficiency in acoustics using SVD," *Journal of Computational Acoustics*, Vol. 14, No. 2, pp. 157-183 (2006).
3. Chen, J. T., Chen, I. L., and Lee, Y. T., "Eigensolutions of multiply-connected membranes using method of fundamental solution," *Engineering Analysis with Boundary Elements*, Vol. 29, No. 2, pp. 166-174 (2005).
4. Chen, J. T., Lee, J. W., and Cheng, Y. C., "On the spurious eigensolution for the real-part boundary element method," *Engineering Analysis with Boundary Elements*, Vol. 33, pp. 342-355 (2009).
5. Chen, J. T., Lin, J. H., Kuo, S. R., and Chiu, Y. P., "Analytical study and numerical experiments for degenerate scale problems in boundary element method using degenerate kernels and circulants," *Engineering Analysis with Boundary Elements*, Vol. 25, No. 9, pp. 819-828 (2001).
6. Chen, J. T., Lin, J. H., Kuo, S. R., and Chyuan, S. W., "Boundary element analysis for the Helmholtz eigenvalue problems with a multiply connected domain," *Proceedings of the Royal Society of London. Series A*, Vol. 457, pp. 2521-2546 (2001).
7. Chen, J. T., Liu, L. W., and Chyuan, S. W., "Acoustic eigenanalysis for multiply-connected problems using dual BEM," *Communications in Numerical Methods in Engineering*, Vol. 20, pp. 419-440 (2004).
8. Chen, J. T., Liu, L. W., and Hong, H. K., "Spurious and true eigensolutions of Helmholtz BIEs and BEMs for a multiply connected problem," *Proceedings of the Royal Society of London. Series A*, Vol. 459, pp. 1891-1924 (2003).
9. Chen, J. T. and Shen, W. C., "Degenerate scale for multiply connected Laplace problems," *Mechanics Research Communications*, Vol. 34, pp. 69-77 (2007).
10. Chen, J. T. and Wong, F. C., "Analytical derivations for one-dimensional eigenproblems using dual boundary element method and multiple reciprocity method," *Engineering Analysis with Boundary Elements*, Vol. 20, pp. 25-33 (1997).
11. Chen, J. T. and Wong, F. C., "Dual formulation of multiple reciprocity method for the acoustic mode of a cavity with a thin partition," *Journal of Sound and Vibration*, Vol. 217, No. 1, pp. 75-95 (1998).
12. Fujiwara, H., *High-Accurate Numerical Computation with Multiple-Precision Arithmetic and Spectral Method*, unpublished report (2007).
13. Golub, G. H. and Van Loan, C. F., *Matrix Computations, 2nd Ed.*, The Johns Hopkins University Press Baltimore, MD (1989).
14. Greenberg, M. D., *Advanced Engineering Mathematics, 2nd Ed.*, Prentice-Hall, Upper Seddle River, NJ (1998).
15 Kuo, S. R., Chen, J. T., and Huang, C. X., "Analytical study and numerical experiments for true and spurious eigensolutions of a circular cavity using the real-part dual BEM," *International Journal for Numerical Methods in Engineering*, Vol. 48, pp. 1401-1422 (2000).
16. Kuttler, J. R., "A new method for caculating TE and TM cutoff frequencies of uniform waveguides with Lunar or eccentric annular cross section," *IEEE Transaction on Microwave Theory and Technique*, Vol. 32, No. 4, pp. 348-354 (1984).
17. Schenck, H. A., "Improved integral formulation for acoustic radiation problem," *Journal of Acoustical Society of America*, Vol. 44, pp. 41-48 (1968).
18. Winkler, J. R. And Davies, J. B., "Elimination of spurious modes in finite element analysis," *Journal of Computational Physics*, Vol. 56, pp. 1-14 (1984).
19. Yeih, W., Chen, J. T., and Chang, C. M., "Applications of dual MRM for determining the natural frequencies and natural modes of an Euler-Bernoulli beam using the singular value decomposition method," *Engineering Analysis with Boundary Elements*, Vol. 23, pp. 339-360 (1999).
20. Yeih, W., Chen, J. T., Chen, K. H., and Wong, F. C., "A study on the multiple reciprocity method and complex-valued formulation for the Helmholtz equation," *Advances in Engineering Software*, Vol. 29, No. 1, pp. 1-6 (1998).
21. Zhao, S., "On the spurious solutions in the high-order finite difference methods for eigenvalue problems," *Computer Methods in Applied Mechanics and Engineering*, Vol. 196, pp. 5501-5515 (2007).